Equivalent Electrical Circuit Derivation of a 7MW Offshore Wind Turbine Gearbox

P. Jaen-Sola*, A. S. McDonald †

Wind & Marine Energy Systems Centre for Doctoral Training, Electronic and Electrical Engineering Department, University of Strathclyde, Royal College Building, 204 George St, Glasgow, G1 1XW, UK

**pablo.jaen-sola@strath.ac.uk; †alasdair.mcdonald@strath.ac.uk*

Keywords: Gearbox, thermal model, parametric loss estimation, equivalent electrical circuit.

Abstract

A thermal model of the main mechanical components of the Levenmouth Development Turbine powertrain has been developed in Matlab/Simulink in order to predict their efficiency curve as a function of torque and speed and their electrical analogues of current and frequency. A parametric loss estimation method has been adapted to the turbine gearbox architecture, its oil type and temperature and used to calculate the load and non-load dependent losses due to bearing, mesh, seal, churning and windage and pump losses. The gearbox losses have been expressed as notional equivalent electrical circuit parameters.

1 Introduction

The next generation of offshore wind turbines will have a wide range of powertrains: direct-drive through to multi-stage gearboxes and induction machines to permanent magnet generators (PMG). The ORECatapult (OREC) 7MW Levenmouth Development Turbine (LDT), is interesting because it has a gearbox and a medium speed PMG; this powertrain topology is becoming increasingly popular for offshore applications (e.g. Adwen, Vestas).
Modern wind turbines use torque control of the generator to track peak aerodynamic performance; the powertrain is designed to deliver this torque control with an appropriate balance of low cost and high efficiency. A significant number of in-service wind turbines operate in sub-optimal conditions [1] due to a number of reasons: component aging, uncertainty in aerodynamic and powertrain parameters, and the control and operational settings not being recalibrated in real time. The inability to recalibrate in real time to account for turbine parameter variations degrades the turbine efficiency, reducing capacity factor and increasing the associated cost of energy. A more dramatic decline is observed in offshore wind farms.

A limited number of studies have centred their attention on a detailed powertrain loss calculation. Basic approximations are typically used by researchers when the gearbox is considered. In [2], the authors state that the gearbox efficiency can vary between 95% and 98% depending on the number of stages and the type of lubrication. In [3], Cotrell suggests that medium speed powertrains are more efficient than conventional high speed arrangements. A 1% per stage approximation due to churning is given for the intermediate and high speed stages. Mesh losses correspond to 0.5% per stage at rated power.
In [4], Polinder *et al* builds on the 1% per stage approximation carried out by Cotrell in [3] but also scales his results according to the rotational speed. Bywaters *et al* [5] and Li *et al* [6] estimated their gearbox losses making use of Cotrell's method.
A more practical approach was developed by Chase *et al* [7] with the aim of testing the efficiency of high speed gearboxes. In [8], the authors analysed mechanical friction losses and windage losses as a function of the rotational speed and certain undefined parameters never disclosed to the public. In [9], Anderson and Loewenthal presented a detailed method to evaluate the efficiency of spur gears. Prakash del Valle in [10] and Duncan in [11] generated simple thermal models in Simulink of small gearboxes without cooling systems. The obtained results were compared with experimental data achieving a reasonable fit.
In industry, complex in-house pieces of software, based on finite element techniques, are produced to estimate the efficiency of the gearboxes [12].

Bearing this in mind, the authors have developed a detailed thermal model in Matlab/Simulink of the main mechanical components of the LDT powertrain to predict their efficiency curve as a function of torque and speed and their electrical analogues of current and frequency, as well as their temperatures. This will allow a comprehensive understanding of the system losses and help increase the capacity factor [13]. The parametric loss estimation method in [14] has been adapted to the LDT gearbox architecture, its oil type and temperature and used to calculate the load and non-load dependent losses due to bearing, mesh, seal, churning and windage and pump losses. The gearbox losses have been expressed as notional equivalent electrical circuit parameters, i.e. three electrical resistances, one dependent on torque, one dependent on rotational speed and one which depends on both. The equivalent electrical circuit reduces complexity and can be easily implemented in full wind turbine models.

2 Gearbox model development

In order to develop a parametric model of the gearbox, the guidelines given in the UK National Standard [14] have been

followed. The symbols and units, as well as the definition of the parameters used in this investigation to calculate the power losses are given in Table 1.

Symbol	Meaning	Units
A_C	Gear casing surface area	m^2
A_g	Arrangement constant for gearing	N/A
a	Load modifying exponent	N/A
b	Diameter modifying exponent	N/A
b_w	Face width in contact with mating element	mm
C_1	Mesh coefficient of friction constant	N/A
D	Outer diameter of gear element	mm
d_i	Bearing bore diameter	mm
d_m	Bearing mean diameter	mm
d_o	Bearing outside diameter	mm
E_p	Electric power consumed	kW
e	Bearing factor	N/A
e_p	Oil pump efficiency	N/A
F_a	Bearing axial load component	N
F_r	Bearing radial load component	N
f_m	Mesh coefficient of friction	N/A
f_0	Bearing dip factor	N/A
f_1	Coefficient of friction for bearings	N/A
f_2	Cylindrical roller bearing factor	N/A
f_3	Bearing seal factor	N/A
f_4	Bearing seal factor	N/A
g	Load intensity modifying exponent	N/A
H_s	Sliding ratio at start of approach	N/A
H_t	Sliding ratio at end of recess	N/A
h	Pitch line velocity modifying	N/A
j	Viscosity modifying exponent	N/A
K	Load intensity	N/mm^2
M	Mesh mechanical advantage	N/A
M_0	No-load torque moment on bearings	Nm
M_1	Bearing load dependent moment	Nm
M_2	Cylindrical roller bearing axial load Dependent moment loss	Nm
M_3	Frictional moment of bearing seal	Nm
n	Rotational shaft speed	rpm
n_1	Pinion rotational speed	rpm
P	Bearing load	N
P_A	Transmitted power	kW
P_B	Total bearing losses	kW
P_{Bi}	Individual bearing load power loss	kW
P_L	Load dependent losses	kW
P_M	Total gear mesh losses	kW
P_{Mi}	Individual loaded mesh power loss	kW
P_N	Non-load dependent losses	kW
P_P	Total oil pump power required	kW
P_{Ps}	Shaft driven oil pump power	kW
P_S	Total oil seal losses	kW
P_V	Heat generated	kW
P_{WB}	bearing windage power loss	kW
P_{WBi}	Individual bearing windage power loss	kW
P_l	Bearing dynamic load	N
p	Operating oil pressure	N/mm^2
Q	Oil volumetric flow	l/min
r_{o1}	Pinion outside radius	mm
r_{o2}	Gear outside radius	mm
r_{w1}	Pinion operating pitch radius	mm
r_{w1}	Gear operating pitch radius	mm
T_1	Torque on the pinion	Nm
u	Gear ratio	N/A
V	Pitch line velocity	m/s

Y, Y_2	Bearing factors	N/A
z_1	Number of pinion teeth	N/A
z_2	Number of gear teeth	N/A
α_w	Operating transverse pressure angle	degrees
β_w	Helix angle	degrees
η	Efficiency	%
v	Kinematic viscosity of oil at room temperature	cSt

Table 1: Symbols and units [14]

By using a model like this, the user can easily estimate the power losses of a particular gearbox with high level of accuracy due to its parametric nature. The three stage epicyclic planetary gearbox of the LDT wind turbine has been considered in this study. Figure 1 shows a sketch of the gearbox arrangement.

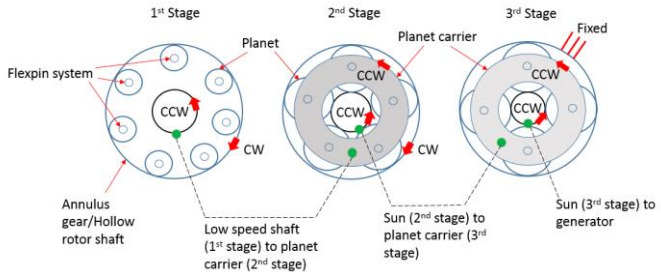

Figure 1: LDT wind turbine gearbox arrangement

As seen, a hollow rotor shaft rotating clockwise acts as a gearbox housing and as the annulus gear for stages 1 and 2. Seven planet gears are mounted onto flexpin systems in the first stage. Planets do not orbit around the sun gear. The flexpins are attached to a back plate, which is bolted to the outer casing. The low speed shaft in the first stage rotates anticlockwise with the same speed as the wind turbine rotor and drives the planet carrier of the second stage. In the second stage there are 5 planet gears mounted onto flexpins. The sun gear, in this case, rotates anticlockwise again and at higher speed than if the annulus would be fixed and drives the planet carrier of the third stage. This second stage creates a superposition. This concept is beneficial in order to achieve high gear ratios. The third stage is rather conventional with a stationary annulus gear and four planets mounted onto flexpins and with the sun gear rotating anticlockwise. The sun gear in the third stage is connected to the electrical generator. The overall gear ratio is 10.7. Further details on the turbine and gears characteristics can be found in Tables 2 and 3, respectively. An oil pump lubrication system driven by one of the reducer shafts was considered. The gearbox was assumed to be fully drained off.

So as to develop a loss model for this machine the guidelines given in [14] have been followed. The thermal rating calculation is based on the fact that the heat generated in a gear drive P_V is equal to the heat dissipation of the gear drive, P_Q. Thus $P_Q = P_V$. The heat generated in a gear drive, P_V, can be estimated by adding up load dependent losses, P_L, and non-load dependent losses, P_N.

$$P_V = P_L + P_N . \quad (1)$$

The load dependent losses are a function of the input power, P_A,

$$P_L = f(P_A). \quad (2)$$

Rearranging terms in Equation (1), the basic heat balance equation can be found,

$$P_Q - P_N - f(P_A) = 0. \quad (3)$$

When Equation (3) is satisfied, the overall efficiency can be estimated as follows,

$$\eta = 100 - \frac{P_L + P_N}{P_A} \times 100. \quad (4)$$

The load dependent losses, P_L, can be calculated using Equation (5),

$$P_L = \sum P_B + \sum P_M \quad (5)$$

where P_B and P_M are the bearing load losses and the mesh losses of the gears, respectively. The non- load dependent losses can be found by summing up the seal losses, P_S, the bearing windage losses, P_{WB}, and the pump losses, P_P.

$$P_N = \sum P_S + \sum P_{WB} + \sum P_P. \quad (6)$$

In order to calculate the gear tooth mesh power losses of an individual gear Equation (7) was utilised. For information about symbols and their units see Table 1.

$$P_{Mi} = \frac{(f_m T_1 n_1 cos^2 \beta_w)}{9549M} \quad (7)$$

The equation to calculate the mechanical advantage, M, is as follows,

$$M = \frac{\left(2cos\alpha_w (H_s + H_t)\right)}{H_s^2 + H_t^2} \quad (8)$$

where the sliding ratio at start of approach, H_s, is calculated using Equation (9),

$$H_s = (u+1)\left[\left(\frac{r_{o2}^2}{r_{w2}^2} - cos^2\alpha_w\right)^{0.5} - sin\alpha_w\right] \quad (9)$$

and the sliding ratio at the end of recess, H_t, is calculated using Equation (10),

$$H_t = \left(\frac{u+1}{u}\right)\left[\left(\frac{r_{o1}^2}{r_{w1}^2} - cos^2\alpha_w\right)^{0.5} - sin\alpha_w\right]. \quad (10)$$

Finally the load intensity, K, is given by Equation (11)

$$K = \frac{1000T_1(z_1 + z_2)}{2b_w(r_{w1})^2 z_2} \quad (11)$$

where f_m, coefficient of friction of the gears was found with Equation (12).

$$f_m = \frac{v^j K^g}{C_1 V^h} \quad (12)$$

For the calculation of the bearing load dependent losses, the load dependent torque, M_1, on each bearing as a function of the applied load is equal to

$$M_1 = \frac{f_1(P_1)^a(d_m)^b}{1000} \quad (13)$$

whereas the axial dependent moment is equal to

$$M_2 = \frac{f_2 F_a d_m}{1000}. \quad (14)$$

The load dependent power loss for an individual bearing can be calculated using Equation (15).

$$P_{Bi} = \frac{(M_1 + M_2)n}{9549} \quad (15)$$

In order to estimate the bearing non-load dependent losses, the frictional moment, M_0, is characterised by two equations depending on the value of the product of the oil viscosity and the rotational shaft speed.
If $vn < 2000$:

$$M_0 = 1.6 \times 10^{-8} f_0 d_m^3 . \quad (16)$$

If $vn \geq 2000$:

$$M_0 = 10^{-10} f_0 (vn)^{2/3} d_m^3 . \quad (17)$$

The frictional moment, M_3, of a bearing sealed at both ends is given by Equation (18)

$$M_3 = \frac{\left(\left(\frac{d_m}{f_3}\right)^2 + f_4\right)}{1000}. \quad (18)$$

The windage power loss for an individual bearing can be calculated using Equation (19).

$$P_{WBi} = \frac{(M_0 + M_3)n}{9549} \quad (19)$$

The oil seal power losses were estimated from Equation (20).

$$P_S = \frac{T_S n}{9549} \quad (20)$$

where $T_S = 3.737 \times 10^{-3} D_s$, with D_s being the diameter of the shaft.
The last type of loss considered was the lubrication oil pump losses, P_{ps}, which was estimated as follows,

$$P_{Ps} = \frac{Qp}{60e_p} \quad (21)$$

2.1 Modelling of external conditions

The loss model was adapted to the characteristics of the LDT wind turbine. The turbine specifications are listed in Table 2. The gearbox input parameters were estimated according to the results achieved from a wind field simulation in QBlade [16]. A 60 seconds simulation was set up considering the rotor radius, hub height, rated wind speed as the mean wind speed, measurement height equal to the hub height, a turbulence intensity of 10% and a roughness length of 0.01m so that the shear layer effect can be included in the study. 60 time steps were assumed (1 per second) with 20 points per direction. Points wind speeds were averaged obtaining a single value for the wind speed in each time step. Then, the rotor speed was found by interpolating between the values given in Table 2, considering that the rotor rotates at 5.9rpm and 10.6rpm when the wind speed is 3.5m/s and 25m/s, respectively. The power corresponding to each time step was acquired by extrapolation, considering the rated power and the rated wind speed. Intermediate and high speed shafts rotational speeds were calculated considering the wind turbine rotor speed and the corresponding gear ratios.

Rated power	7MW
Rotor diameter	171.2m
Hub height	110.6m
Rated wind speed	11.5m/s
Wind speed	3.5 – 25m/s
Rotor speed	5.9 – 10.6rpm
Powertrain	Medium speed (400rpm)
Overall gear ratio	10.7

Table 2: Wind turbine specifications [15]

2.2 Thermal model development in Matlab/Simulink

The development of the complete thermal model of the LDT gearbox implied the creation of a code in Matlab [17], which governs the behaviour of the entire model in Simulink and allows the user to take into consideration distinct features, such as oil degradation with temperature, forces acting on helical gears or to implement a cooling/heating system. The fundamental characteristics of the gearbox components, such as gears or bearings mass, surface area, thermal conductivity, specific heat and density, have been estimated using the SolidWorks (ISO standard) toolbox [18]. All the gears were CAD generated using the data provided in Table 2 so that the unknown characteristics could be found. Shafts, planet carriers and bearings were also CAD generated using the said toolbox, although the data used were appropriate approximations made by looking at the dimensions of the gears and their rotational speeds.

Gear element	No. teeth	Mate teeth	External diameter (mm)
Annulus gear (1st)	260	52	3000
Planet gear (1st)	52	260	805
Annulus gear (2nd)	260	120	3000
Planet gear (2nd)	120	260/20	500
Sun gear (2nd)	20	120	220
Annulus gear (3rd)	260	123	3000
Planet gear (3rd)	123	260/14	1250
Sun gear (3rd)	14	123	160

Table 3: Gear specifications

Double-row cylindrical roller bearings with full complement were assumed for the main bearings (low speed, intermediate speed and high speed), as well as for the flexpin systems. So as to consider the oil degradation, oil viscosity variation with temperature data, as given in [19], were plotted and a trend line fitted. The result obtained is well represented by Equation (22)

$$v = 2785\exp(-0.045T_{\text{sump}}) \quad (22)$$

where T_{sump} is the temperature of the oil. For the creation of the model in Simulink [17], thermal mass blocks were necessary to represent the gearbox elements (gears, bearings, shafts, oil reservoir, air cavity and outer casing). According to the type of heat transfer, conduction (solid-solid), convection (solid-fluid) or radiation (solid-fluid) blocks have been used. These are joint to the corresponding gearbox components simulating the transfer of heat. The changing power losses, are also connected to the thermal masses through ideal heat source blocks. Sensors are placed all over the gearbox to measure the temperatures of every component. The atmosphere has been simulated by using an ideal temperature source block with a constant input temperature of 294K.

The oil cooling/heating system, which starts working when the oil temperature reaches a designated value, was generated using ideal heat source blocks governed by Equations (23) and (24)

$$heating_{\text{gain}} = n \times Q_{\text{heating}} \times \rho_{\text{water}} \times C_{\text{pwater}} \quad (23)$$

$$cooling_{\text{gain}} = n \times Q_{\text{cooling}} \times \rho_{\text{air}} \times C_{\text{pair}} \quad (24)$$

where Q_{heating} is the water volumetric flow, ρ_{water} corresponds to the water density and C_{pwater} to water's heat coefficient, whereas, Q_{cooling} is the air volumetric flow, ρ_{air} corresponds to the air density and C_{pair} to air's heat coefficient. The results for the total power losses and the oil temperatures with and without cooling systems are depicted in Figure 2.

As observed, the total power losses are maximum at 32 seconds, coinciding with the maximum wind speed (11.98m/s). This represents a loss of 1.3% at this particular moment, with the non-load dependent losses accounting for 0.35% and the load dependent losses for 0.95%. From Figure 2(b)(c), it can be understood how the model accurately simulates the effect of the cooling system, as a smooth control of the temperature is achieved.

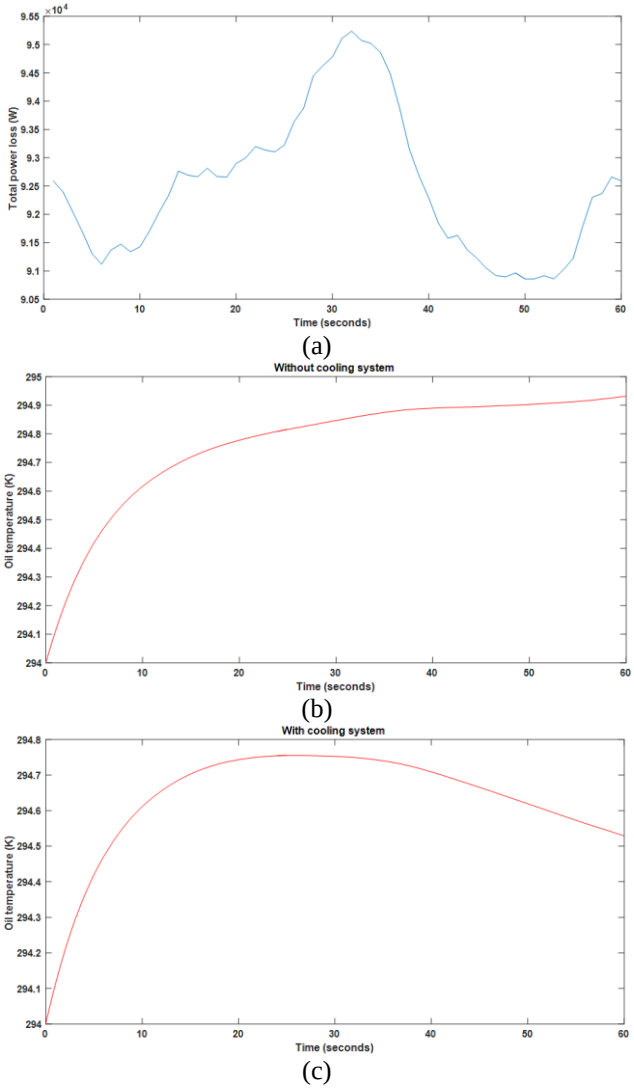

Figure 2: (a) Total power loss "P_V"; (b) Oil temperature vs. time without cooling system; (c) Oil temperature vs. time with cooling system

2.3 Gearbox equivalent electrical circuit derivation

Once the thermal model was completed, the results retrieved from the simulation were analysed and depending on the influence of each variable (in this case torque and rotational

speed are of interest) on the power losses, the power losses were classified into three different categories: torque dependent, rotational speed dependent and torque and rotational speed dependent. By knowing the power losses and the current flowing, electrical resistances can be estimated ($R= P/I^{2)}$, e.g. R_1 (torque dependent), and introduced. For the rotational speed dependent losses, the resistance can be directly added to the variable resistance R_2/s, which depends on a slip, which can be defined in terms of the turbine rotor speed, and hence upon the speed of the generator. In the case of the power losses dependent of both the torque and the rotational speed these can be approximated and separated into components R_1, R_2 and R_3. See Figure 4.

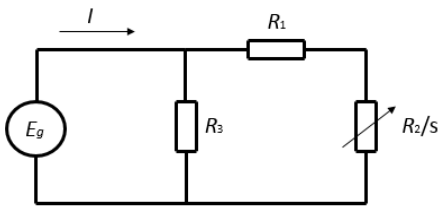

Figure 4: Equivalent electrical circuit of the gearbox

3 Discussion and conclusions

The thermal model development of the LDT gearbox will help understand the system losses. By considering the thermal behaviour of the powertrain mechanical components, the turbine control strategy can be adapted in order to maximize the energy capture. In addition, with the creation of the equivalent electrical circuit of the gearbox the overall complexity of the system is considerably reduced and full wind turbine studies could be carried out by introducing a simplified generator and converter equivalent electrical circuits.

References

[1] G. Hughes, "The Performance of Wind Farms in the United Kingdom and Denmark", Renewable Energy Foundation, London (UK), 2012.

[2] T. Burton, D. Sharpe, N. Jenkins and E. Bossanyi. "Gearbox Efficiency" in The Wind Energy Handbook, 2nd ed. Chichester, United Kingdom: John Wiley and sons Ltd, 2011, Page 437.

[3] J. Cotrell, "A preliminary evaluation of a multiple-generator drive train configuration for wind turbines." In 21st American Society of Mechanical Engineers (ASME) Wind Energy Symposium. 2002.

[4] H. Polinder, F.F.A. Van der Pijl, G-J. De Vilder, and P.J. Tavner. "Comparison of direct-drive and geared generator concepts for wind turbines." in Energy conversion, Volume 21, no. 3, September 2006, Pages 725-733.

[5] G. Bywaters, V. John, J. Lynch, P. Mattila, G. Norton, J. Stowell, M. Salata, O. Labath, A. Chertok, and D. Hablanian. "Northern Power Systems WindPACT drive train alternative design study report." NREL, Golden, Colorado, Report no. NREL/SR-500-35524 (2004).

[6] H. Li, Z. Chen and H. Polinder. "Optimization of multibrid permanent-magnet wind generator systems." in Energy Conversion, Volume 24, no. 1, March 2009, pages 82-92.

[7] D.R. Chase. "Development of an efficiency test methodology for high-speed gearboxes" Electronic Thesis. Ohio State University, 2005. [Online] Available: http://rave.ohiolink.edu/etdc/view?acc_num=osu1209661381. Last Accessed 01/05/2018.

[8] J. Tamura. "Calculation Method of Losses and Efficiency of Wind Generators" in International Conference on Power Electronics and Drives Systems, Volume 2, 28 november-01 December 2005, Pages 1595 – 1600.

[9] N.E. Anderson and S.H. Loewenthal. "Spur-Gear-System Efficiency at Part and Full Load" NASA, Cleveland, Ohio, Report no. NASA TP-1622 (1980).

[10] C. Prakash Del Valle, "Thermal Modelling of an FZG Test Gearbox," MSc Thesis, KTH Industrial Engineering and Management, Stockholm (Sweden), 2014.

[11] D. Morrison, "Thermal Modelling of a Wind Turbine Gearbox with a View to Condition Monitoring," MSc Thesis, University of Strathclyde, Glasgow (UK), 2017.

[12] RomaxWIND, https://www.romaxtech.com/software/romaxwind/, [Online] Last Accessed 01/05/2018.

[13] J.P. Echenique, "Improving the Performance of a Wind Energy System", Ph.D. dissertation, The University of Edinburgh, Edinburgh (UK), 2015.

[14] Anon., "Gears —Thermal capacity —Part 1: Rating gear drives with thermal equilibrium at 95°C sump temperature". BSi, Report no. BS ISO/TR 14179-1:2001 (2001).

[15] ORE Catapult Levenmouth research wind turbine data, provided at Supergen WIND hub annual meeting, University of Strathclyde, May 2016.

[16] QBlade documentation, http://www.q-blade.org/, [Online] Last Accessed 01/05/2018.

[17] Matlab/Simulink help documentation, https://uk.mathworks.com/help/simulink/index.html, [Online] Last Accessed 01/05/18.

[18] SolidWorks help documentation, http://help.solidworks.com/, [Online] Last Accessed 01/05/18.

[19] Shell Omala S4 GX 320 synthetic industrial gear oil technical data sheet, http://hand.net.pl/wp-content/uploads/2014/02/GPCDOC_GTDS_Shell_Omala_S4_GX_320_en_TDS.pdf, [Online] Last Accessed 01/05/18.